An Experiment in Earthquake Control at Rangely, Colorado

C. B. Raleigh, J. H. Healy, J. D. Bredehoeft

The discovery in 1966 that injection of fluid underground at high pressure was responsible for the triggering of earthquakes near Denver, Colorado, led to speculations that earthquakes might be controllable (1). Reduction of the frictional strength of the highly stressed basement rock by injection of the fluid is the favored explanation for the mechanism by which the earthquakes were triggered (2). The pressurized fluid enters a fracture and supports a part of the normal stress equivalent to the pressure of the fluid. As the fluid has no shear strength, the *effective* normal stress and the frictional resistance to sliding are lowered. If the fracture is subject to shear stress greater than the product of this effective normal stress and the coefficient of friction, the rocks will slip and generate an earthquake. This hypothesis was not uniformly accepted by earth scientists, and although supported by the available data the hypothesis could not be established conclusively at Denver.

The injection of waste fluid into the Army's disposal well at the Rocky Mountain Arsenal was discontinued in 1966, and the earthquakes have now almost completely ceased. The disposal well, because of its proximity to Denver, could not be used for experimental purposes, but the experience was nevertheless highly significant. Earthquakes apparently were being triggered by injection of fluid into stressed rock, and with reduction in fluid pressure the earthquakes sharply decreased in frequency. If the physical basis for these phenomena could be well established in a field experiment, earthquake control and prevention of inadvertent triggering of earthquakes might become feasible.

For an adequate field experiment it was necessary (i) to know the fluid pressure in the vicinity of the hypocenter of the earthquakes, (ii) to measure the absolute state of stress, (iii) to have precise hypocentral locations and focal plane solutions for the earthquakes, and most important (iv) to be confident that the active phase of the experiment would not materially increase the likelihood of a damaging earthquake. In 1967 we were advised by W. W. Rubey that the Rangely Oil Field might meet our requirements. An array of seismographs at Vernal, Utah, had been recording small earthquakes from the vicinity of Rangely since its installation in 1962 (3). The field had been on waterflood—the injection of water at high pressure for secondary recovery of oil—since 1957. In the fall of 1967, we installed a portable array of seismographs and recorded 40 small earthquakes in a 10-day period at the Rangely field (4). The earthquakes occurred within the oil field in two areas where fluid pressures due to waterflooding were high. In 1968, the leaseholders and the operator, Chevron Oil Company, agreed to permit us to conduct an experiment to control the seismic activity in a part of the field. The experiment began in September 1969 with the full cooperation of Chevron and was supported by the Advanced Research Projects Agency of the Department of Defense, who were interested because the Army's well at Denver had triggered the earthquakes there.

The experiment was planned as follows. After a year of recording of seismic activity from a local network of seismographs, the fluid pressure in the vicinity of the earthquakes would be reduced by backflowing water from injection wells. If the fluid pressure reduction resulted in reduced seismic activity, the pressure would be raised again by injection and the cycle repeated. Concurrent measurements of reservoir pressure in nearby wells would be used to establish the reservoir performance and make predictions of the spatial distribution of pressure with the cycles of injection and withdrawal. By measuring the stresses in situ and the frictional properties of the reservoir rock, a test of the effective stress hypothesis could be made by comparing the observations with the predicted fluid pressure for triggering of earthquakes.

The Rangely Field

The Rangely structure consists of a doubly plunging anticline in Mesozoic and Paleozoic sedimentary rocks (Table 1 and Fig. 1a). The Cretaceous Mancos shale is exposed at the surface, and is underlain at 900 m below the surface by an 800-m section of Mesozoic sandstones and siltstones. The Pennsylvanian and Permian Weber sandstone, the principal oil reservoir rock, is 350 m thick and is encountered at a depth of about 1700 m. The Paleozoic sandstones and limestones beneath the Weber rest on crystalline basement rock at a depth of about 3000 m.

There is little evidence of faulting in the Rangely area. At the western end of the field, drainage patterns are aligned along a structure trending 30° east of north (N 30° E) that produced 500 m of apparent displacement in rocks 5 km north of the oil field. There is no evidence of displacements on this fault where its projection to the south intersects the rocks along the south flank of the fold. In the subsurface, the depths to the top of the Weber sandstone within the field permit continuous structural contours to be drawn, except in one area, where a fault is required (Fig. 1a). Along an east-northeast trend through the center of the field, variations in depth to the Weber could be accounted for by a fault with an apparent vertical displacement of 10 to 15 m. The steeper dips on the southern flank of the fold make it difficult to trace the fault off to the southwest. Although there is no subsurface evidence from the steeper southwest flank of the fold, the fault is dashed to the southwest on the contour map (Fig. 1a) because of the presence of fractures and calcite veins having an east-northeast trend in the Mancos shale in this area (5). Less than 1 km south of the oil field boundary, however, no displacement in dipping units of the outcropping Mesaverde formation can be detected along the projected trace of the fault. Either the fault was inactive after deposition of the Mancos, or the displacement within the weak Mancos shale was distributed over a broad zone. In any case, the fault, which is the principal seismically active structure at Rangely, is quite a modest one; it would have gone undetected if it were not within an oil field.

The Weber sandstone is a dense, fine-grained sandstone with an average porosity of 12 percent and an average permeability of 1 millidarcy in the oil-producing zone. Consequently, despite the large estimated reserves, the reservoir pressure and production rate declined rapidly following development of the field in 1945. In 1957, the field was divided into units to fa-

C. B. Raleigh and J. H. Healy are geophysicists at the National Center for Earthquake Research, U.S. Geological Survey, Menlo Park, California 94025. J. D. Bredehoeft is a hydrologist at the U.S. Geological Survey, Reston, Virginia 22092.

cilitate waterflooding to increase the productivity. After this, wells on the periphery of the field were converted to water injection. By 1962, pressure surveys (6) showed that in local areas injection had raised the reservoir fluid pressures above 170 bars, the virgin reservoir pressure. By 1967, when earthquakes were first accurately located in the field, bottom-hole pressures as high as 290 bars were recorded.

Seismicity

Before the installation of the Uinta Basin Seismic Observatory at Vernal, Utah, there were no instrumental records of earthquakes at Rangely. We were given one secondhand report of felt earthquakes in the area from the period before fluid injection, but we have not attempted to verify the report. Continuous recording from the U.S. Geological Survey network, which permitted the first accurate location of earthquakes, began in October 1969, 12 years after waterflooding was begun. Thus, we are unable to establish any correlation between the initiation of waterflooding and the onset of seismic activity at Rangely. Nevertheless, a correlation between seismicity and high pore pressure was established as soon as a clear pattern of earthquake activity emerged from analysis of the data from the microearthquake network (Fig. 1b).

Table 1. Subsurface rocks in the Rangely Oil Field.

Formation	Thick-ness (m)	Depth (m)
Mancos shale	990	990
Dakota sandstone	93	1083
Morrison formation	223	1306
Curtis formation	30	1336
Entrada sandstone	43	1379
Carmel formation	23	1402
Navajo sandstone	160	1562
Triassic (undifferentiated)	273	1835
Park City formation	43	1878
Weber sandstone	408	2286
Pennsylvanian upper member of Morgan formation	102	2388

A seismic network consisting of 14 short-period, vertical seismometers was installed in 1969 and the data telemetered to Menlo Park. The network was maintained in essentially the same configuration during the period of the experiment to avoid any problems that might arise from changing the number of stations or the instrumentation. As the data were analyzed systematically by a small group of people, and most were examined by one person, there are no inconsistencies resulting from changes in staff or in analysis procedures.

Because the zone in which we were able to control the fluid pressure in this experiment is not large, the location of the earthquakes is critically important for establishing the relationship between fluid pressure and seismicity. Procedures have been developed to determine the parameters of a flat-layered velocity model from a set of earthquake data in a dense network of seismograph stations. If horizontal velocity gradients exist, systematic errors will be present in the earthquake locations calculated from a flat-layered model. It turned out that a systematic bias does exist in the standard locations, which moves earthquakes toward the north.

To determine the parameters of a flat-layered model that would fit the data, we used a linear velocity function approximated for computation by 0.5-km-thick layers. The parameters of this model were varied to minimize the residuals—differences between the measured and calculated compressional wave arrival times—in a set of 100 earthquakes, and a station correction was determined for each station that would compensate for variations in near-surface structure.

Two people independently picked the arrival times for the set of earthquakes, and two independent locations were determined by using the Hypolayr routine (7). The histogram of the horizontal distances between these pairs of locations (Fig. 2) provides an estimate of the random errors in the location procedure. Some of the pairs of locations were separated by more than 400 m, but most were closer than 200 m.
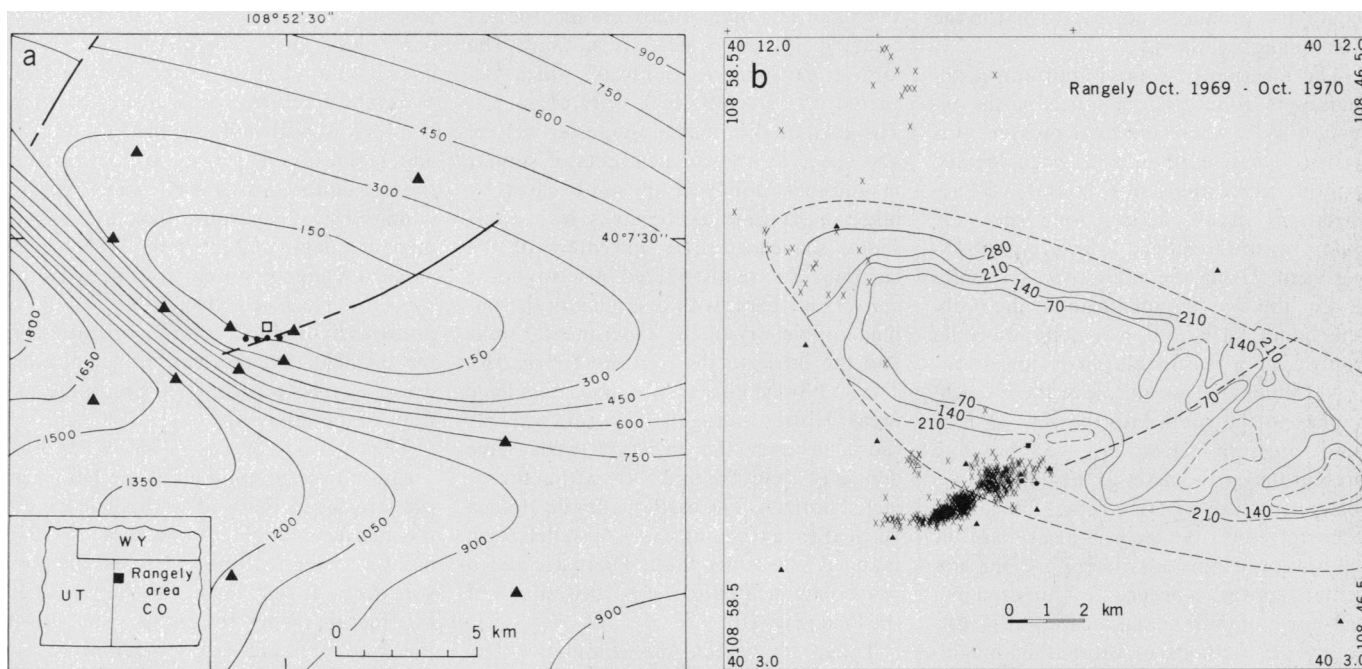
The velocity model derived from the

Fig. 1. (a) Structure contour map of the Rangely anticline with subsurface faults shown as dashed lines. The contour interval is 150 m, indicating depth below sea level to the Weber sandstone. (●) Experimental wells used for varying fluid pressure in Weber sandstone. (□) Well used for measurement of stress. (▲) Seismic stations. (b) Earthquakes (x) located at Rangely between October 1969 and November 1970. The contours are bottom-hole 3-day shut-in pressures as of September 1969; the interval is 70 bars. (▲) Seismic stations; (●) experimental wells. The heavy, dashed line indicates the fault mapped in the subsurface.

earthquake data was a good approximation to the velocity measured in a well in the center of the oil field, and earthquakes located with this model had residuals that were of the same magnitude as the probable error in the measured arrival times (0.01 to 0.02 second).

Lateral variations in the velocity-depth profile cannot be easily detected from the earthquake data alone, and lateral variations in velocity can result in a systematic bias in location. To test for such a bias, a calibration shot was fired at a depth of 2000 m in one of the injection wells. The signals from the shot were well recorded on most of the regular stations and on a supplementary network installed to record the shot. The calculated location of the shot fell 200 to 300 m north of the actual location, depending on which combination of stations was used to locate it. The most distant stations did not record the shot, and it is probable that lateral trends in velocity would produce a greater offset in the location if data from the distant stations were available.

The pressure changes in the Weber sandstone brought about by the removal of fluid from the center of the field and injection of water around the edges of the field are large enough to produce a significant change in velocity. Measurements of velocity in the Weber sandstone as a function of effective confining pressure indicate that a change as large as 5 percent is possible (8). The distribution of the pressure changes with respect to the seismic zone would also produce a northward bias in the earthquake locations.

The location of some important earthquakes is about 500 m north of the injection wells where the fluid pressure was varied. These earthquakes, when located without corrections for lateral velocity variation, actually lie in a zone where the fluid pressure remained low during the experiment. Using the calibration shot data and qualitative judgments about the probable lateral variations in velocity, we could apply a set of reasonable corrections to the travel times that would move these earthquakes to the south into the zone of high fluid pressure. However, we chose to present the earthquakes as located by a velocity structure with isotropic, flat layers, uncorrected for the error in location of the calibration explosions. Therefore, the epicenters appear to occur a few hundred meters north of their actual location (Fig. 6).

Several methods of estimating magnitude were tested, and a method based on the duration of the seismic signal was found to be the most systematic and reliable. The duration of the signal was independent of the distance of the quake from
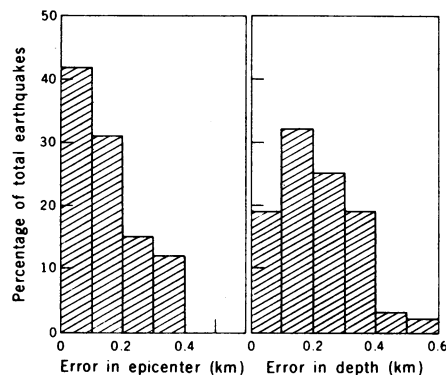

Fig. 2. Relative errors in epicentral and depth locations of 100 earthquakes due to differences between the first arrival readings made by two separate observers.

the station, and all but a few stations gave a consistent measure of duration (t in seconds) that was related to magnitude by $M = 1.8 \log t - 1.0$. Stations that were anomalous with respect to the average were not used in the estimate of magnitude. The accuracy of any measure of seismicity depends entirely on the precision of the estimated magnitudes of the smallest earthquakes used in the count. Different cutoff magnitudes were examined, and no systematic bias was observed that could be related to inaccuracies in magnitude. Earthquakes with a coda length of more than 2 seconds were located, and all located earthquakes were used in the seismicity statistic.

The magnitudes of the Rangely earthquakes chosen for study are $M_L \geq -0.5$. Events of this magnitude were recorded as clear signals on at least six stations. The largest earthquakes, both of which occurred on 21 April 1970, were $M_L = 3.1$. The earthquakes tended to cluster in time and space as swarms of events of similar magnitudes, followed in some cases by larger-magnitude earthquakes with aftershock sequences. The epicenters of the earthquakes are distributed into two dense clusters in space, with one lying in the immediate vicinity of the experimental wells and the other to the southwest (Fig. 1b). The southwest cluster of hypocenters have focal depths averaging 3.5 km, whereas those beneath the injection wells have depths of about 2.0 to 2.5 km within the injected horizon. The earthquakes lie along a vertical zone trending nearly parallel to the mapped subsurface fault. There are also a few events located in the northwest end of the field (Fig. 1b).

Taken altogether, the cumulative frequency relative to magnitude of the Rangely earthquakes fits the equation log $N = a + bM$. If the two clusters of earthquakes are treated independently, the value of b for the deeper, southwesterly clus-

ter is 0.81; that for the northeasterly cluster is 0.96.

Focal plane solutions derived from the radiation pattern of compressional wave arrivals have been generated for a large number of individual earthquakes. The distribution of the azimuths of the nearly vertical nodal planes is bimodal, with one peak parallel to the trend of epicenters shown in Fig. 3. The nodal planes parallel to the epicentral trend and the subsurface fault correspond to fault planes with a right-lateral sense of shear, having a slip direction plunging 10° to 20° to the southwest (Fig. 3). The fault can therefore be considered to be a right-lateral, approximately strike-slip fault. The variations in the orientations of the nodal planes may represent real differences in the orientations of rupture surfaces rather than errors due to inaccuracies in the locations of the earthquakes. The width of the epicentral zone is more than 1 km, or three times the error in the relative locations of the epicenters. It appears that the fault is not a single, large fracture surface, but a broad zone composed of subparallel fractures.

Effective Stresses

To test the hypothesis that increased fluid pressure triggered the earthquakes at Rangely by reducing the effective normal stresses on the fault surfaces, we attempted to measure the absolute stresses and the orientation of the fault planes and slip directions. Hydraulic fracturing of rock in boreholes affords a method to measure the in situ state of stress. The theory relating hydraulic fracturing pressure to the stress in rocks is well understood (9), and field and laboratory experiments confirm that the technique works well under certain conditions. A hydraulic fracture experiment at a depth of 2 km in the Weber sandstone at Rangely was carried out by Haimson (10). He had shown from records of previous hydraulic fracturing operations in the oil field that the least principal compressive stress was constant over large sections of the reservoir.

The method consists of increasing fluid pressure in a borehole until the hoop tensile stresses in the wall of the hole exceed the tensile strength of the rock. At that point a tensile fracture opens and the pressure drops as fluid flows into the propagating fracture. When the pump is shut down, the fluid pressure drops precipitously as fluid from the borehole continues to flow into the fracture. When the fracture closes, the fluid pressure flattens out at a value (the instantaneous shut-in pressure) equivalent to the normal stress acting

across the crack surface. In theory and experiment (11) the crack propagates normal to the least principal compressive stress. The shut-in pressure is equal to the least principal stress, S_3, and the maximum principal stress, S_1, is given by the relation

$$P_f = T + 3S_3 - S_1 - P_0$$

where T is the tensile strength and P_0 the preexisting fluid pressure in the rock. The breakdown pressure is P_f. The experiment at Rangely was carried out in unfractured rock of low permeability, 0.1 millidarcy, and yielded a vertical tensile fracture oriented N 70° E.

Laboratory experiments have shown that the breakdown pressure is a function of the rate of pressurization of the borehole in the laboratory specimen (10). Consequently, experiments were performed on cores of Weber sandstone to measure breakdown pressure under known stresses and different rates of pressurization, to determine the appropriate value of T. The pressurization rate at Rangely was 3 bars per second. At comparable pressurization rates in the experiments the tensile strength was about 100 bars. The exact rate is not important; in this range of pressurization rates, the breakdown pressure is insensitive to the rate. A specimen in which the internal hole was sealed with sealing wax also yielded a value of 100 bars, indicating that the permeability of the Weber sandstone is not a significant factor in the breakdown pressure at such pressurization rates (12).

The hydraulic fracture in the reservoir yielded the following values of the stresses. Given a measured value of 162 bars for P_0, the initial fluid pressure in the rock, a shut-in pressure of 314 bars, and a breakdown pressure of 328 bars, then $S_1 = 552$ bars, $S_2 = 427$ bars (the overburden stress), and $S_3 = 314$ bars.

From the orientation of the fault and slip direction determined from focal plane solutions of nearby earthquakes (13), the shear and normal stresses resolved into the slip direction and normal to the fault plane, respectively, are $\tau = 72$ bars and $S_n = 342$ bars. The coefficient of static friction, μ, for faulted specimens of Weber sandstone (14) is 0.81. Applying the Hubbert-Rubey failure criterion to faulting at Rangely

$$\tau_c = (S_n - P_c)\mu.$$

where τ_c is the shear stress at failure, S_n is the normal stress, and P_c is the critical fluid pressure required to trigger earthquakes, gives $P_c = 257$ bars as the critical fluid pressure above which earthquakes should be triggered.

The orientations of the maximum and

minimum principal stresses are consistent with those of the stresses measured at or near the surface at several localities within 50 km of Rangely (15). The approximately east-west orientation of the regional maximum compressive stress is consistent with the mode of faulting as revealed by the fault zone trending about N 50° E. If stresses generated by the steep fluid pressure gradients in the field (Fig. 1b) were responsible for triggering the earthquakes, the sense of slip would be left- rather than right-lateral as observed. The principal test of the triggering mechanism is the effect on the seismic activity of lowering and raising

the fluid pressure with respect to the 257-bar value calculated above. Our original calculation of the predicted triggering pressure was published in 1972 (13). It was not until the period December 1972 to May 1973 that a complete cycle of raising and lowering the fluid pressure around this value could be achieved.

Reservoir Fluid Pressures

Periodically a bottom-hole pressure survey is made throughout the Rangely field in an attempt to map the pressure distribu-
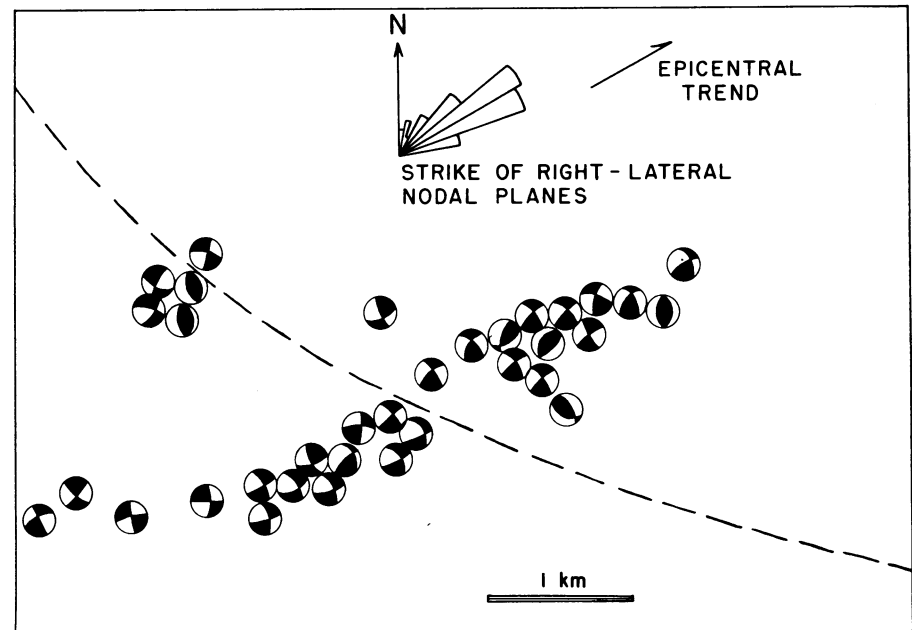

Fig. 3. Compressional wave radiation patterns of Rangely earthquakes shown on lower hemisphere equal-area projections. Black is the first motion up, white the first motion down. The rose diagram shows azimuths of right-lateral nodal planes. The dashed line shows the southern boundary of the oil field.
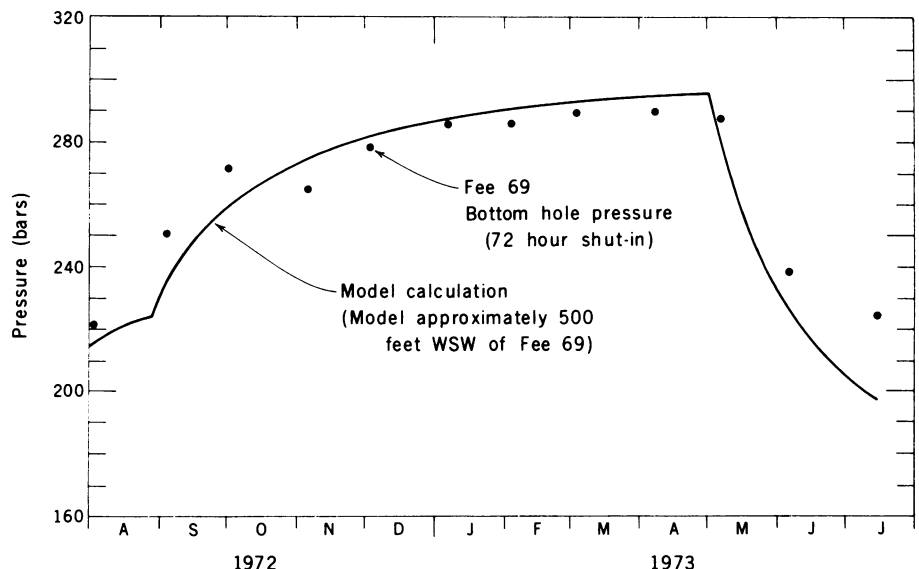

Fig. 4. Bottom-hole fluid pressures observed in experimental well Fee 69 compared with pressures calculated from reservoir simulator model at a distance of 150 m west-southwest of the well.

tion in the Weber reservoir. To obtain representative reservoir pressures, a well is shut in and pressures are measured over a period of several days, then extrapolated to "undisturbed" reservoir pressures. After the field was unitized in 1957, these surveys were made annually; in recent years the surveys have been made every 2 years. The Weber reservoir pressure distribution measured by the field's operators in 1969 (Fig. 1b) is typical of the recent pressure distribution in the oil field. A reservoir simulation model was developed to provide a more detailed picture of the pressure distribution in the part of the oil field used in this experiment. The model is used to solve the basic partial differential equations for reservoir pressure by a finite-difference approximation method (16, 17).

Three phases—oil, gas, and water—have existed in the oil field. A gas cap that was present in the area of interest was removed in the first stages of production. Because we were only interested in calculating reservoir pressures, we simulated the reservoir by a single-phase model, but used a variable compressibility in an effort to compensate for the effects of the variations in the oil/water ratio. The producible fluid now in the area of earthquake activity is water.

The bottom-hole pressure measurements fit the adjusted model rather well. In particular, the observed pressure history (Fig. 4) in well Fee 69 (Fig. 5) fits the calculated history closely.

Reservoir pressures were continuously monitored at the surface in five shut-in wells near the zone of earthquake activity; these observation wells are indicated in Fig. 5. Pressure transducers were installed at the wellheads and data were transmitted to a central recorder at well Emerald 45, which is located 400 m west of the experimental wells. These data were supplemented with the monthly bottom-hole pressures taken in the same wells (Fig. 5).

Two of the instrumented wells, UPRR 29-32 and UPRR 67-32, are close to the fault zone to the northeast. These wells are less than 800 m from the zone of earthquake activity, and neither well shows a marked change in reservoir pressure that can be correlated with pressures in the active area (Fig. 5). This suggests that the fault to the northeast of the active area is not a zone of unusually high permeability along which pressure changes are rapidly transmitted. The transmissibility (effective permeability) of this general part of the reservoir is approximately 15,000 to 30,000 millidarcy-centimeters. Using the reservoir model, we experimented with anisotropic permeability along the fault zone, making the fault zone two, three, and five times more permeable parallel to the fault. The
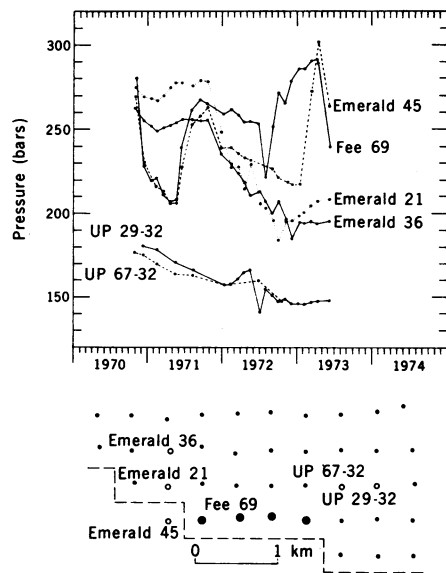

Fig. 5. Pressure history and map showing observation wells. Experimental wells are indicated by large closed circles.

factor of 5 for anisotropy gave the best results.

In contrast to the wells to the northeast, Emerald 45, which is 0.75 km due west of the active earthquake zone, responds very rapidly to pressure changes in the active area. For most of the period the correlation in pressure between wells Fee 69 and Emerald 45 is quite striking (Fig. 5). During the period December 1971 to March 1973 the casing in Emerald 45 was leaking, and because of the leak the pressures are not correlated during this period. After the casing leak was fixed, in March 1973, the pressure in Emerald 45 again approached and closely followed the pressure in Fee 69. Emerald 45 must be closely connected, presumably by a fracture or system of fractures, to the zone influenced by the injection wells. That such rapid communication of fluid pressures can take place indicates that it may be possible to quickly effect pressure variations in fractures within the fault zone.

Reservoir pressures at selected times in the experiment were calculated for comparison with the earthquake activity (Fig. 6a). The pressure distribution is shown only on the epicenter maps that cover the part of the field of interest. The vertical distribution of pressures is not known, and no attempt is made to represent the fluid pressure in the vertical cross sections in Fig. 6b. The 72-hour shut-in pressures measured at the bottom of well Fee 69 are taken as representative of the fluid pressures in the earthquake zone, at least in that part of the zone underlying the four injection wells. These shut-in pressures are compared with a histogram showing the frequency of seismic events in Fig. 7.

Controlling the Earthquakes

From October 1969 to 10 November 1970, injection into the four designated wells raised the bottom-hole pressure in the vicinity from 235 to 275 bars (Figs. 5–7). During that time, more than 900 earthquakes occurred in the field, 367 of them within 1 km of the bottom of the four injection wells. On 10 November the wells were shut in for 3 days and then backflowed. The record of pressure in Fig. 5 shows the monthly 72-hour shut-in pressures taken at well Fee 69 dropping from 275 to 203 bars in 6 months. Seismic activity within 1 km of the wells dropped from the previous year's average of 28 earthquakes per month to about 1 per month. On 26 May 1971 reinjection was initiated, and the bottom-hole pressure at Fee 69 was raised to 265 bars. The seismic activity near the wells remained at less than 1 earthquake per month.

In September 1971 the pattern of waterflooding in the Rangely field was changed to increase production of oil, and the wellhead injection pressures in the experimental area decreased as a result. The bottom-hole pressures then declined gradually until August 1972, when a booster pump was installed to raise the pressures back to at least the original value of 275 bars. Between October 1972, when the bottom-hole pressure first exceeded the predicted critical value of 257 bars, and January 1973, when the pressure had risen to 275 bars, the monthly average of earthquakes near the wells rose to six. From January until the end of April, with the pressure standing at about 280 bars, the monthly average of earthquakes near the wells was 26. The wells were shut in and backflowing was begun on 6 May 1973. Since that day no earthquakes have been recorded within 1 km of the bottom of the four injection wells, and only one earthquake per month has been recorded along the fault zone to the southwest.

Discussion and Conclusions

The experiment at Rangely has confirmed the hypothesis that earthquakes may be triggered by increase of fluid pressure and has shown that the effect is well accounted for by the Hubbert-Rubey principle of effective stress. The strong temporal correlation between frequency of the seismic activity and variations in the fluid pressure around the predicted value is evidence for this conclusion. The frictional strength of the fault varies in direct proportion to the difference between the total normal stress and the fluid pressure. This result comes as no surprise; the effect of

1234

pore pressure on brittle failure in rock has been verified repeatedly in laboratory experiments. However, given the complexities of a real fault zone, with dimensions scaled up by four to five orders of magnitude relative to laboratory specimens, it is especially significant that successful prediction of the approximate pore pressure required for triggering of earthquakes according to the Hubbert-Rubey theory was possible. In order for this to be so, several requirements had to be met.

It was necessary to know the complete state of stress and the distribution of fluid pressure at the depth of the earthquake hypocenters. The conditions for use of the hydraulic fracturing technique for stress measurement were nearly ideal. Moreover, the method could be applied economically at the depth where the earthquakes occurred because of the active drilling program in the oil field.

Permeability to fluid flow along the fault is sufficiently large that adjustment of fluid pressure in the fault follows rapidly upon changes in fluid pressure at the experimental wells. The cessation of seismic activity within 1 day of the initiation of backflowing the experimental wells in May 1973 established the correlation between fluid pressure and earthquakes beyond reasonable doubt. A large lag between fluid pressure changes in seismic activity would have necessitated several repetitions of the injection-withdrawal cycle.

Extraction of oil (and injected water) just to the north of the experimental wells served to maintain fluid pressures over most of the fault zone well below the critical value for triggering earthquakes. Therefore, the length of the fault zone liable to shear failure was so limited that earthquakes of damaging size were virtually precluded. It is this safety feature that leads us to believe that earthquakes triggered inadvertently by raising subsurface fluid pressures in otherwise seismically inactive areas can be controlled. By making use of the strengthening effect of a reduction of fluid pressure in a major fault zone, we may ultimately be able to control the timing and the size of major earthquakes.

Limiting the magnitudes of earthquakes. Although fluid injection for secondary recovery of oil or brine disposal has not, to our knowledge, triggered damaging earthquakes, the procedure is becoming extremely widespread, involving, in a few cases, injection near large active faults. Moreover, filling of several large reservoirs has been accompanied by severe earthquakes (*18*), probably through leakage of the impounded water into faults. In either case, with knowledge of the location of the fault on which the seismic activity is induced, drilling and pumping of pore fluid

from the fault zone could serve to reduce the hazard.

The Rangely experiment has brought the possibility for control of naturally occurring earthquakes into sharp focus. We now know that faults, at least in the shallow crust, obey a simple failure law in which fluid pressure plays a clearly under-

stood role. The fault can be strengthened locally by reducing the internal fluid pressure, thereby creating a barrier to the propagation of a rupture. Provided the barriers so created are spaced at distances of one to a few kilometers apart, the fractures can be limited to lengths appropriate for earthquakes of less than damaging size.
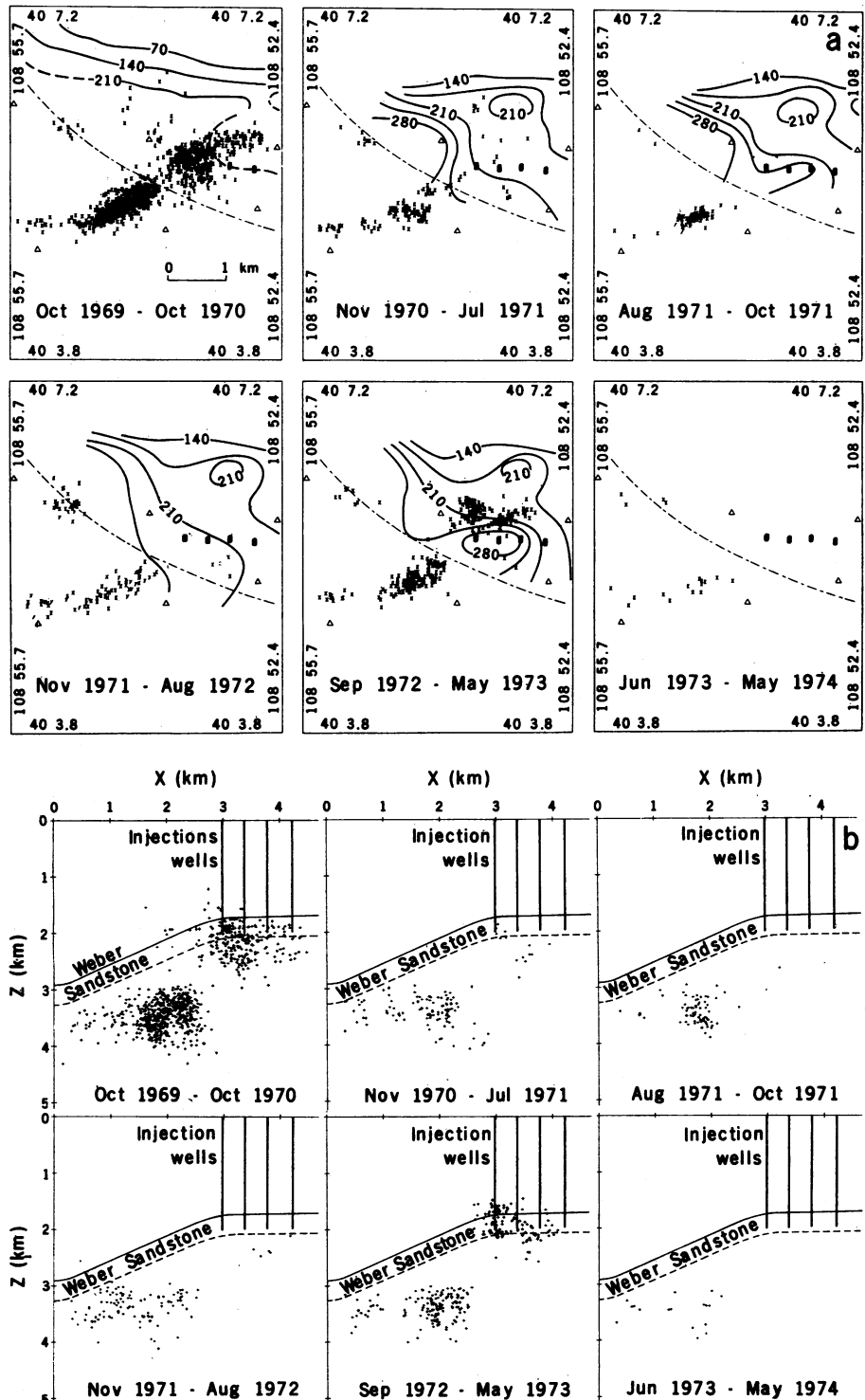

Fig. 6 (a) Seismicity at Rangely for different intervals of time. Pressures (bars) were calculated for the reservoir at the times indicated, except for the map for October 1969 to October 1970, where the contours are from bottom-hole pressures measured in September 1969. (b) Vertical sections looking north, showing earthquakes as a function of time. The injection horizon, the Weber sandstone, and the four experimental wells are shown.
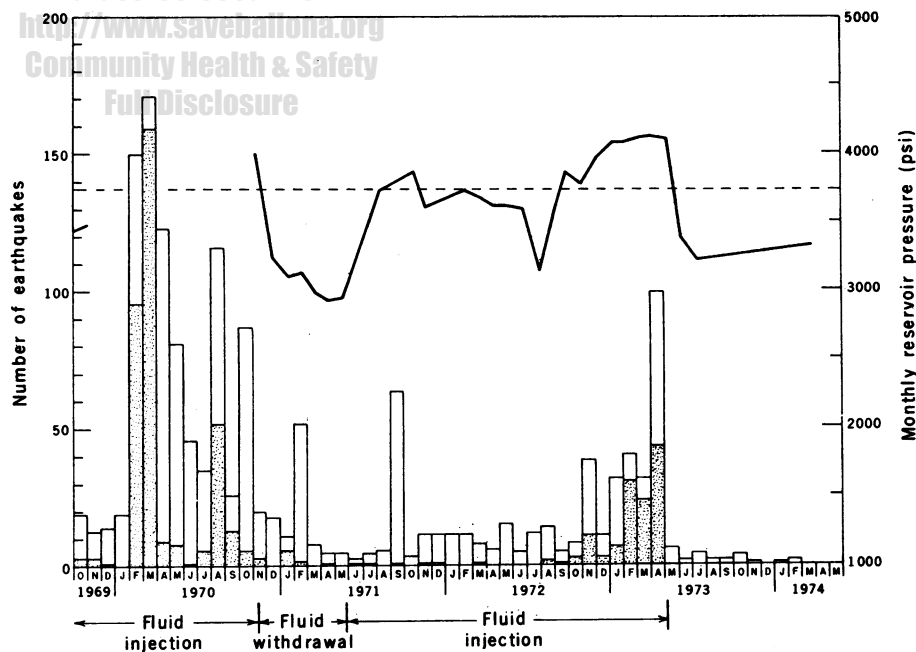
Fig. 7. Frequency of earthquakes at Rangely. Stippled bars indicate earthquakes within 1 km of experimental wells. The clear areas indicate all others. Pressure history in well Fee 69 is shown by the heavy line; predicted critical pressure is shown by the dashed line.

along critical sections of the San Andreas fault would provide data necessary to evaluate the feasibility of controlling the behavior of this dangerous fault. Many hypothetical problems have been conceived that would preclude the possibility of ever obtaining any degree of useful control over a great fault, and it is possible that a few exploratory holes would demonstrate that attempts to control the San Andreas fault would be either too dangerous or too expensive. But, given the encouraging results of the research reported in this article, we feel that control of the San Andreas fault could ultimately prove to be feasible. A more complete study of the fault may reveal properties that might simplify the technical aspects of control. The recent rapid advances in research on the mechanisms of earthquakes, combined with the Rangely results, lead us to the conclusion that initial experiments preliminary to control of earthquakes on the San Andreas fault should now be carried out.

Summary

An experiment in an oil field at Rangely, Colorado, has demonstrated the feasibility of earthquake control. Variations in seismicity were produced by controlled variations in the fluid pressure in a seismically active zone. Precise earthquake locations revealed that the earthquakes clustered about a fault trending through a zone of high pore pressure produced by secondary recovery operations. Laboratory measurements of the frictional properties of the reservoir rocks and an in situ stress measurement made near the earthquake zone were used to predict the fluid pressure required to trigger earthquakes on preexisting fractures. Fluid pressure was controlled by alternately injecting and recovering water from wells that penetrated the seismic zone. Fluid pressure was monitored in observation wells, and a computer model of the reservoir was used to infer the fluid pressure distributions in the vicinity of the injection wells. The results of this experiment confirm the predicted effect of fluid pressure on earthquake activity and indicate that earthquakes can be controlled wherever we can control the fluid pressure in a fault zone.

Various schemes can be conceived which would lead to reduction of the size of earthquakes. For example, the San Andreas fault has an average slip rate of 2 to 3 cm per year (19). We wish to accommodate the slip without permitting the strain to accumulate to yield great earthquakes every 100 to 200 years. An earthquake of magnitude 4.5 requires a fault length of about 5 km and yields 2 cm or so of slip. In one scheme of earthquake control, wells are drilled 5 km apart and 5 km or so in depth, and the fluid pressure is reduced by the required amount and over the required area of the fault to arrest a fracture of this size. Another well is drilled in the center of each 5-km section, and fluid is injected to trigger an earthquake (Fig. 8). Now, in the faulted area the stress is relieved, but concentration of stress results at the ends of the fracture in the strengthened zones. Next, fluid is pumped out of the wells formerly used for injection, and this zone becomes strengthened. The fluid is then injected into the intervening wells, and new earthquakes are triggered at the former barriers so that the accumulated stress is relieved. The procedure must be alternated at intervals of 6 months to accommodate the required slip rate. Dieterich, who has contributed much to this discussion, has developed a laboratory analog of this model (20).

Whether such a scheme is feasible depends on several factors, which presently are unknown. The permeability of the fault zone is chief among these. Should we find that there are extensive sections of rock in the fault that have very low permeability,

removal of fluid to render the zone effective as a crack arrester would require an uneconomically large number of wells. There are no data on the permeability of the fault zone at depths where earthquakes occur. Nor do we know the temperature, the existing state of stress or pore pressure, or much about the material properties of the fault zone. Except for conducting laboratory studies and developing case histories of other earthquake sequences related to fluid pressure increases, there is little that can be done at this time in research on earthquake control until those quantities are measured.

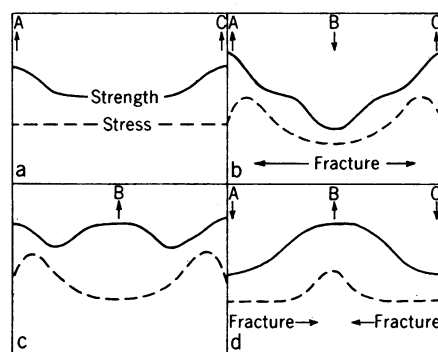A few holes 7 km or so in depth drilled

Fig. 8. Hypothetical scheme for controlling earthquakes. (a) Fluid is removed from wells A and C, with an increase in frictional strength along the fault. (b) Fluid is injected into well B, triggering an earthquake; the stress drops at B and increases at A and C, where the fracture is arrested. (c) Fluid is removed from well B, resulting in an increase in strength at B. (d) Fluid is injected at A and C, producing earthquakes, and the fracture is now arrested at B.

References and Notes

1. D. Evans, Mt. Geol. 3, 23 (1966).
2. J. H. Healy, D. T. Griggs, W. W. Rubey, C. B. Raleigh, Science 161, 1301 (1968).
3. R. C. Munson, thesis, Colorado School of Mines (1968).
4. J. F. Gibbs, J. H. Healy, C. B. Raleigh, J. M. Coakley, Bull. Seismol. Soc. Am. 63, 1557 (1973).
5. C. R. Thomas, Map of the Rangely Oil and Gas Field, Rio Blanco and Moffat Counties, Colorado (Oil and Gas Investigations No. 41, U.S. Geological Survey, Washington, D.C., 1945).
6. E. Klipp, personal communication.

7. J. P. Eaton, "HYPOLAYR," *U.S. Geol. Sur. Open-File Rep.* (1969).
8. R. Stewart, personal communication.
9. R. O. Kehle, *J. Geophys. Res.* **69**, 259 (1964).
10. B. C. Haimson, *Proc. 14th Symp. Rock Mech.* (1972), p. 689.
11. M. K. Hubbert and D. G. Willis, *Trans. AIME* **210**, 153 (1957).
12. The apparent increase in breakdown pressure at high pressurization rates is related to the inability of the viscous fluid to reach the tip of the propagating crack (M. Zoback, F. Rummel, R. Jung, H. Alhied, personal communication). The pressure in the borehole will, therefore, continue to rise rather than show a sudden flattening out with time.

13. C. B. Raleigh, J. H. Healy, J. D. Bredehoeft, *Geophys. Monogr. Am. Geophys. Union 16* (1972), pp. 275–284.
14. J. D. Byerlee, *Int. J. Rock Mech. Min. Sci. Geomech. Abstr.* **12**, 1 (1975).
15. C. B. Raleigh, in *Advances in Rock Mechanics* (National Academy of Sciences, Washington, D.C., 1974), vol. 1, part A, pp. 593–597.
16. D. W. Peaceman and H. H. Rachford, Jr., *J. Soc. Ind. Appl. Math.* **3**, 28 (1955).
17. G. Pinder and J. D. Bredehoeft, *U.S. Geol. Surv. Water Resour. Div.* **4** (No. 5), 1069 (1968).
18. H. K. Gupta, B. K. Rastogi, H. Narain, *Geophys. Monogr. Am. Geophys. Union 17* (1973), pp. 455–467.

19. R. E. Wallace, *Geol. Soc. Am. Bull.* **81**, 2875 (1970).
20. J. H. Dieterich and C. B. Raleigh, *Eos* **55**, 353 (1974).
21. We wish to acknowledge the excellent work of J. Bohn and L. Peake in reading and analyzing the seismic records from Rangely. Our colleagues J. D. Byerlee, J. H. Dieterich, and J. Handin contributed significantly to this work. D. T. Griggs and W. W. Rubey encouraged us to begin this experiment and gave valuable advice and support over the 5 years required to complete it. We received valuable advice from a panel appointed by the Advanced Research Projects Agency. The work was carried out under ARPA order 1684.

Restored Pictures of Ganymede, Moon of Jupiter

Digital restoration of two space pictures of Ganymede has revealed some interesting surface features.

B. Roy Frieden and William Swindell

Ganymede is the largest moon of Jupiter, having a diameter of about 5000 km. Because earth-based telescopes can barely resolve it, the details of Ganymede's surface are largely unknown. Other, nonvisual evidence has led to the belief that its surface is very rough, largely composed of rocky or metallic material embedded in ice (*1*). The detailed pictures presented here provide a body of visual information on the surface makeup of Ganymede.

During its mission to Jupiter, the Pioneer 10 spacecraft acquired two pictures of Ganymede (*2*), which provided a much improved view of its surface. The pictures were obtained with two different color filters, one in red (5950 to 7200 Å) and one in blue (3900 to 5000 Å). Unfortunately, these pictures are quite blurred because of the small scale of details on Ganymede relative to the size of the image blur spot (the total instrument response function).

We report here the results of an attempt to restore the pictures—that is, to remove the blur due to the instrument response function. Such removal is at least theoretically possible, because the instrument response function is deterministic, and largely known.

The authors are professors of optical sciences at the University of Arizona, Tucson 85721.

Let $s(x,y)$ represent the instrument response function, with x,y the usual space coordinates. Mathematically, the restoration problem consists in inverting the imaging equation

$$i(x_m,y_n) = \iint\limits_{scene} dx'dy'\,O(x',y') \times$$
$$s(x_m - x', y_n - y') \qquad (1)$$
$$m,n = 1,2,\ldots,M$$

for the unknown $O(x',y')$, the "restoration." The irradiance image data $i(x_m,y_n)$ and response function $s(x,y)$ are assumed known, from measurements, and hence contain noise. Such noise is the chief impediment to estimating $O(x',y')$.

Three factors aided in making such restoration practicable. First, the irradiance image is a linear function of the image data; hence, there are no problems of estimating the irradiance image such as occur when the image is photographic.

Second, and most important, the image was sampled at a sufficiently fine subdivision to allow some degree of enhancement. There were about 28 sampled image values within the central core of the two-dimensional instrument response function.

Third, the instrument response function is very nearly separable. That is, if $s(x,y)$ represents the general response function,

with x,y the usual space coordinates, in our case

$$s(x,y) \simeq s_1(x)s_2(y) \qquad (2)$$

Functions s_1 and s_2 are the x- and y-component marginal distributions of s. Although Eq. 2 is an approximation, the maximum discrepancy between the left- and right-hand sides is about 2 percent of the central maximum in s. Figure 1 shows the marginal imaging kernels s_1 and s_2.

Separability is important because it permits use of a restoration procedure—the maximum entropy algorithm—whose output is constrained to be positive (or zero) everywhere (*3*). The general two-dimensional case would otherwise require too much computer time. Because of separability, the two-dimensional image may be restored as a sequence of one-dimensional, or line, restorations. These may be implemented with enough speed to permit the positive constraint to be enforced on the moderate-sized Ganymede pictures discussed below.

One negative aspect of the problem was the occasional existence of artifacts in the image data. Even worse, the artifacts were systematic—that is, highly correlated—and hence indistinguishable from true detail. We discuss below the steps we took to minimize this problem.

The images were restored in two different ways: by conventional linear filtering and by the maximum entropy algorithm cited above. To the best of our knowledge, the latter is the first published use of this kind of algorithm on real (nonsimulated), moderately extended image data.

The linear restoring algorithm was of the type used by Nathan (*4*)—inverse filtering, with a maximum permitted boost in amplitude specified by the user. Phase was always fully corrected. All operations on the image data were in direct (compared to frequency) space. Hence, the image was restored by convolution with a function whose Fourier transform is the upper-bounded, inverse filter. We tried maximum boosts of 2, 4, 5, and 10 before settling on 2 as the most reliable.